Chemical Engineering and Processing 68 (2013) 69–73

Contents lists available at SciVerse ScienceDirect

Chemical Engineering and Processing: Process Intensification

journal homepage: www.elsevier.com/locate/cep

Dip coating with colloids and evaporation

Guillaume Berteloot[a], Adrian Daerr[a], François Lequeux[b], Laurent Limat[a,*]

[a] Laboratory MSC, Matière et Systèmes Complexes, UMR 7057 of CNRS and University Paris Diderot, 10 rue Alice Domon et Léonie Duquet, F-75013 Paris, France
[b] Laboratory SIMM, Science et Ingéniérie de la Matière Molle (formerly PPMD), UMR 7615 of CNRS and ESPCI, 10 rue Vauquelin, F-75005 Paris, France

ARTICLE INFO

Article history:
Received 17 November 2011
Received in revised form 27 July 2012
Accepted 4 September 2012
Available online 11 September 2012

Keywords:
Coating
Colloids
Moving contact line
Wetting and evaporation
Drying

ABSTRACT

We investigate the coating of a glass plate with silica colloids by a dip coating method in presence of evaporation. We show experimentally that the deposed quantity plotted versus plate velocity V exhibits a minimum, in agreement with a simple argument developed by us in a previous, theoretical paper. This minimum corresponds to a crossover between the well-known Landau–Levich regime observed at higher plate velocity and a less well-known regime at lower plate velocity where the deposit is formed directly at the contact line. This very general result is consistent with experiments and calculations made by other teams with different compounds or under different drying geometries. Modifying our initial argument by taking into account the particle density gradient, we show that a simple modeling of each regime in terms of scaling laws is possible, the deposed mean thickness scaling respectively as V^{-1} and $V^{2/3}$ in the lower and higher velocity limits.

1. Introduction

There is a growing interest in coating hard and soft substrates with colloids, because of numerous applications to optics and microelectronics [1,2]. A possibility to realize these substrates is to use dip coating under evaporation [3], i.e. to remove at constant speed a plate from a bath of colloidal suspension while drying occurs. This leads to several undesired effects: defects, heterogeneous deposition, cracks and delamination [1,4]. The problem is also difficult to model as three singularities may coexist at the contact line (CL) receding on the substrate [5,6] (and even in a advancing case [7]): (1) divergence of viscous stresses, (2) divergence of evaporation as in the well known "coffee stain" effect [8–10], (3) and divergence of colloid concentration. In a recent paper we modeled the hydrodynamics in the vicinity of a moving, evaporating, contact line [5], and we found that there should exist two different regimes at respectively low and high plate velocity: in these two regimes, the deposed mean thickness e should respectively decrease and increase with the plate velocity V, the high velocity limit following a classical Landau–Levich scaling of the kind $e \sim V^{2/3}$. This should lead to a minimum of the deposit thickness for a critical intermediate velocity. If we except a very recent study performed with complex compounds on silicium in extreme conditions [11], this effect has been scarcely evidenced in a dip coating experiment with colloids, though similar behaviors were found for deposition of phospholipids [12], and in a different two-plate geometry (meniscus receding in a Hele-Shaw cell) [13,14]. More recently, a similar minimum was found in a dip coating experiment assisted by forced air convection [15], which confirms the great generality of this behavior.

We present here evidences in favor of this effect in the case of silica colloids deposited on glass from water solutions with dip coating [6]. Our experimental conditions are described in Section 2, and the results presented in Section 3, where we also compare the entrained thickness to the standard Landau–Levich argument [16]. To summarize, we found that the deposition is perturbed by complex behaviors (stick-slip and instability) that strongly alter the uniformity of the deposit, but despite this additional complexity the two predicted regimes indeed appear with this minimum of deposed thickness at their crossover. In Section 4, we remind our qualitative modeling of hydrodynamics near the deposition front of Ref. [5], that leads at low plate velocity to a thickness decreasing with velocity, i.e. to this minimum, and in Section 5, we include the effect initially neglected by us of the particle concentration gradient. We show that this additional term modifies the predictions in the limit of low plate velocity ("evaporative" regime), for which the deposed thickness scales as $e \sim V^{-1}$ instead of $e \sim V^{-2}$, as initially suggested in [5,6]. These predictions are in good agreement with our data and with others obtained on different systems [11–15,17,18]. Let us note here that the V^{-1} law has been proposed very early by Dimitrov and Nagayama [17] and rediscovered later independently by Diao and Xia [18], and by Jing et al. [14] who interpreted it on the basis of a balance of solvent at the scale of the meniscus. As we shall see both arguments (our's and the

* Corresponding author.
E-mail address: laurent.limat@univ-paris-diderot.fr (L. Limat).

0255-2701/$ – see front matter © 2012 Elsevier B.V. All rights reserved.
http://dx.doi.org/10.1016/j.cep.2012.09.001

solvent balance at the meniscus level) are equivalent, the interest of our approach being that scaling laws are also provided for the spatial dependency of particle concentration during deposition. This could allow one to build future extensions to situations involving several independent length scales, or to prepare further experimental investigations of these spatial effects with – for instance – fluorescent microscopy.

2. Experiment and general observations

A sketch of the experimental set-up is suggested in Fig. 1a. A clean glass plate is plunged inside a colloidal suspension and removed from this bath at constant speed (V ranging between $50\,\mu m\,s^{-1}$ and $5\,cm\,s^{-1}$), while deposition and evaporation takes place on the glass. We used silica suspensions (Klebosol silica slurries 50R50, 30R25 and 30R12) with three different particle diameters (12 nm, 25 nm and 50 nm), and two different mass fractions (ϕ_m = 5% and 10%). The glass plate is cleaned and prepared before each experiment by the following protocol. First the glass surface is rubbed with an abrasive cerium oxide suspension (concentration 20%), cleaned with pure water, ethanol, and again pure water, and then let to dry. A plasma treatment is then imposed to the glass. After these treatments, the two sides of the glass plate display a nearly total wetting behavior with water, the effective observed contact angle θ_S not exceeding a few degrees.

After drying completion, the deposit has been observed with an atomic force microscopy (AFM), and by optical profilometry. A typical example of an AFM visualization is reproduced in Fig. 1b, and several views with optical profilometry in Fig. 1d–f). The particles are deposed in a random way, with many defects at small scale, and the spatial distribution at large scale is also scarcely uniform, perturbed by a disordered patterning linked to stick-slip of the effective contact line and to instabilities of the entrained suspension film. However, it is possible to define four main kinds of deposition, whose range of plate velocity values are indicated in Fig. 2b. At low velocity (Fig. 1d), the deposit is perturbed by a stick-slip effect, similar to the one observed by Rio et al. [7] on advancing contact lines of colloidal suspensions, or by Ghosh et al. [19] and Bodiguel et al. [13] for receding contact lines. At intermediate velocities (Fig. 1e), the deposit is reasonably uniform, or at least continuous, before to be again perturbed by film flow instabilities at high plate velocity (Fig. 1f) of unknown origin. At very low velocity the deposit delaminates, as shown on the side view reproduced in Fig. 1c.

3. Mean thickness deposed and Landau–Levich limit

Initially, we measured the mean thickness of the deposit, using these profilometry records, versus plate velocity for the different particle sizes and concentrations. While this method gives us a first idea of the shape of the deposit it has two significant drawbacks: a reference point is needed (i.e. we need to have naked glass on the image to have a reliable measurement) and the field of view is limited to a few millimeters. In addition, these two combined constraints lead to measurements in the immediate vicinity of the initial contact line, where transitional regimes are most likely to happen.

We then relied on a more averaged method consisting in weighing the substrates before and after the experiment. Using a balance of accuracy 1 mg, and producing coated domains of typical extent $15\,cm \times 8\,cm$ on each side of the plates, we were able to measure the mass per unit surface of the deposit μ with an accuracy of order $7 \times 10^{-5}\,kg/m^2$. The results are displayed in Fig. 2b, where two distinct regimes separated by a minimum of the thickness are clearly visible, in good agreement with our theory [5,6]. To be more quantitative, we have plotted on the same graph the law that could be expected in the "high" velocity limit from a Landau–Levich argument. In the higher velocity range, the plate entrains a continuous film of liquid out of the bath, that dries later on the whole extent of the plate. As well known from available literature [3], the thickness of the liquid film e is equal to that calculated long ago by Landau, Levich and Derjaguin [16], and should scale as $e = 0.94\,l_c {Ca}^{2/3}$ where $Ca = \eta V/\gamma$ designates the Capillary Number built upon liquid viscosity η, plate velocity V, surface tension γ, and where $l_c = \sqrt{\gamma/(\rho g)}$ is the capillary length (g acceleration of gravity, ρ mass density of the liquid). During drying, the volume fraction occupied by the particles in the liquid increases from the initial volume fraction ϕ_0 to a critical value close to the maximal packing concentration ϕ_c, which implies that the deposit thickness observed at high velocity should read:

$$e_{HV} = 0.94 \frac{\phi_0}{\phi_c} l_c \left(\frac{\eta V}{\gamma}\right)^{2/3} \tag{1}$$

Accordingly, the mass deposited per unit surface on the plate should read:

$$\mu = 0.94 \rho \phi_m l_c \left(\frac{\eta V}{\gamma}\right)^{2/3} \tag{2}$$

where ϕ_m is mass fraction of particles in the bulk of the solution. This prediction is plotted on the log–log plot in Fig. 2b (continuous line), where we have used the known values for water of the following quantities: $\eta \approx 10^{-3}$ Pa s, $\rho \approx 10^3\,kg/m^3$, $\gamma \approx 80$ mN/m. There are strong fluctuations of our measurements that were averaged over only two realisations, but the results are sufficient to support a 2/3 exponent at high plate velocity and to confirm a change of regime at low plate velocity, with the formation of the expected minimum close to a critical velocity of order $0.1\,mm\,s^{-1}$ here. It seems difficult to define an exponent in this regime from our data, but considering its distribution, the -1 value reported by other teams seems more reasonable than our initial guess -2 of Ref. [5].

Surprisingly, the quantity of particles deposited on the plate in the Landau–Levich regime is four or five times larger than predicted by the prefactor deduced from pure water properties. Also, though the data have been normalized by the initial bulk mass fraction of particles, the points obtained for the largest fraction are systematically below those obtained for the other. These two trends suggest that the influence of particle concentration gradients are not negligible in our situation, even in the high velocity limit.

4. Modeling

We now remind the physical origin of the two very different behaviors suggested by the two sketches in Fig. 2a and c, and provide the reader with a qualitative modeling of the "evaporative" regime observed at low velocity. As explained above, at high velocity a Landau–Levich film is pulled out of the bath, and dries on the plate, leading to expressions (1) and (2) for the deposed thickness and mass. At low velocity (see the sketch in Fig. 3a), the situation is very different. There is now a contact line, from which the deposit directly emerges, evaporation being now mainly localized at the contact line itself. Following Deegan et al. [8,9], the evaporating flux diverges there, following a law of the kind (see Fig. 3a):

$$J = \frac{J_0}{x^{1/2}} \tag{3}$$

where J_0 can be estimated here by noting that at the scale of the meniscus size x_∞ ($x_\infty \sim 2l_c$, l_c capillary length with the notations of Fig. 2) the mean evaporating velocity should be given by:

$$\frac{J_0}{\sqrt{x_\infty}} \propto \frac{D}{x_\infty} \frac{c_{sat}}{\rho} \tag{4}$$

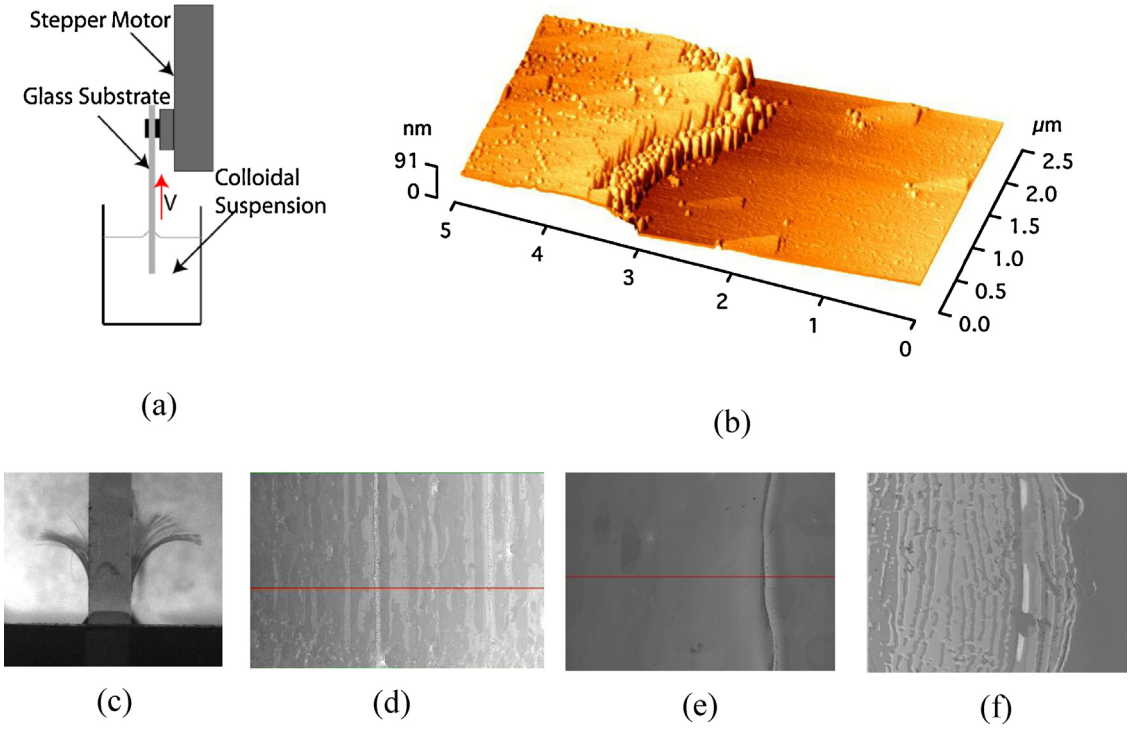

Fig. 1. (a) Experimental set up. (b) A typical AFM visualization of the deposit. (c) Delamination observed at very low plate velocity (the plate thickness, viewed here from the side, is 5 mm). (d–f): Deposit left on the plate after drying, observed by optical profilometry, for increasing plate velocity: (a) $V = 50\,\mu m\,s^{-1}$, (b) $V = 1\,mm\,s^{-1}$, (c) $V = 5\,cm\,s^{-1}$. The motion of the plate took place along the horizontal direction of the pictures. The particle mass fraction was equal to 10%, and the particle size (not visible here) was equal to 50 nm. The horizontal scale of these pictures is of order 3 mm (total extent of the pictures).

where D is the diffusivity of water in air, c_{sat} the saturation mass concentration of water vapour in air, supposed to be reached at the free surface of the liquid (and to vanish at infinity), and ρ the mass density of water. Using the classical values for water evaporating in air, $D = 24 \times 10^{-6}\,m^2\,s^{-1}$, $c_{sat} = 24 \times 10^{-3}\,kg\,m^{-3}$, $\rho = 10^3\,kg\,m^{-3}$ and $x_\infty \approx 2\,mm$, one gets typically $J_0 \approx 10^{-9}\,cm^{3/2}\,s^{-1}$.

There are now two effects that will be superimposed in the selection of the deposit thickness. First, the evaporation field will induce a hydrodynamic flow that will drive the particle toward the contact line where these ones will be deposed, and also, this flow, combined with evaporation will modify the particle concentration near contact line. We successively discuss both aspects in the two following

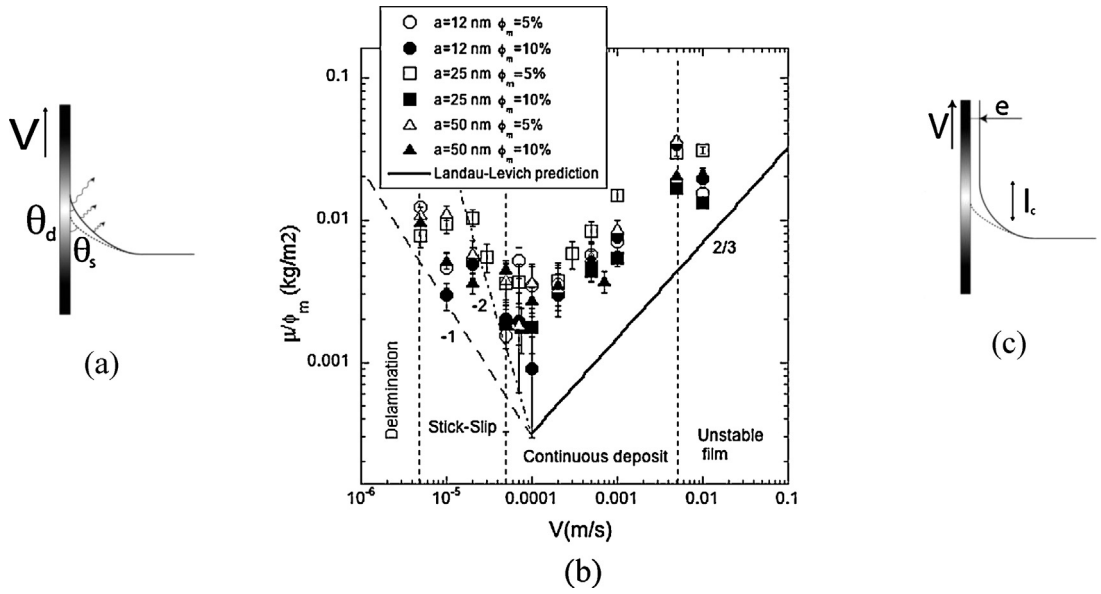

Fig. 2. Mass of silica colloids per unit surface μ deposed on a glass plate by dip coating, normalized by the initial particle mass concentration ϕ, for two concentrations and three particle sizes (b). Roughly, two regimes of deposition appear, the one on the right (c) being linked to the entrainment of a Landau–Levich film at high plate velocity, the other on the left (a) with deposition and evaporation directly at the contact line. The continuous line is the exact result expected from Landau–Levich, while the two discontinuous lines, of respective slope −1 and −2 are guides for the eyes.

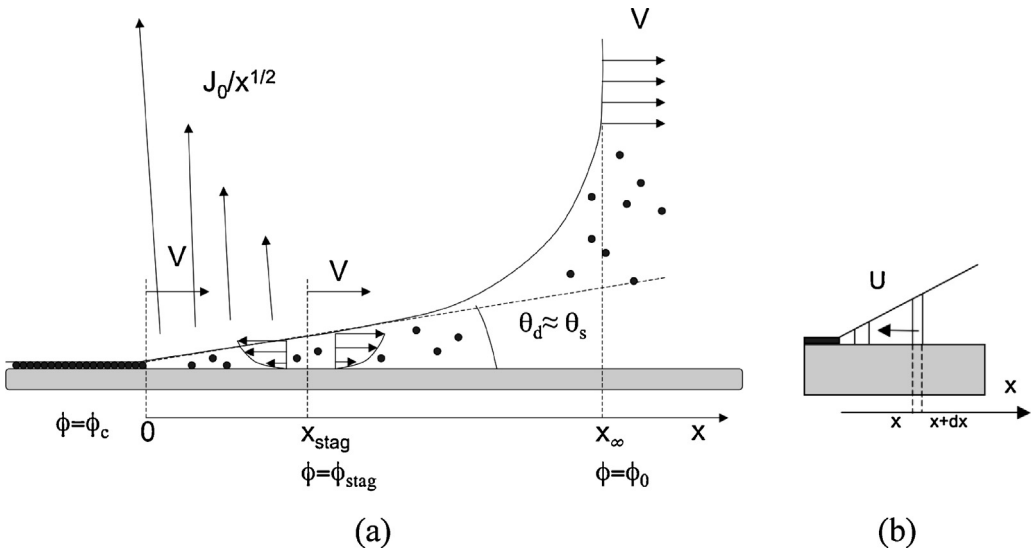

Fig. 3. (a) Sketch of the low velocity problem in the framework of the plate, treated here as static, the liquid receding to the right. (b) During its motion toward contact line, the volume of a slab of liquid is changing because of evaporation, which introduces a change of particle concentration.

parts, before addressing the possible influence of colloid diffusion in the very last one.

4.1. Hydrodynamics of deposition

In the framework attached to the plate, the liquid motion should obey the following mass conservation equation:

$$-V\frac{\partial h}{\partial x}+\frac{\partial}{\partial x}[h<u_x>]=-\frac{J_0}{\sqrt{x}} \tag{5}$$

where $\langle u_x\rangle$ designates the mean velocity averaged on the liquid thickness $h(x)$, given in the lubrication approximation by: $\langle u_x\rangle = -(h^2/3\eta)(\partial P/\partial x)$, with $P = P_{atm} - \gamma(\partial^2 h/\partial x^2)$, P_{atm} being the reference atmospheric pressure. Integrating one time this equation leads to a mean velocity

$$\langle u_x\rangle = V - \frac{J_0}{2h(x)}\sqrt{x} \tag{6}$$

that exhibits a stagnation surface located at a distance to the contact line equal to:

$$x_{stag} = \left(\frac{J_0}{2\theta_d V}\right)^2 \tag{7}$$

where θ_d is the dynamic contact angle, supposed to be rather close to the static angle θ_S in this low velocity limit. The structure of the flow is suggested in Fig. 3a. For scales $x < x_{stag}$ evaporation drives everything to the contact line, and in particular all the colloids trapped in this region. We thus guess that x_{stag} will play the role of a capture length ruling the thickness deposited on the plate in the low velocity limit e_{LV}. To estimate it, a balance of solute can be written as follows: the plate is withdrawing from the liquid a volume per unit of length and unit of time of solute equal to $Ve_{LV}\phi_c$, while the stagnation surface crosses a volume of solute equal to $V\theta_S x_{stag}\phi_{stag}$, where ϕ_{stag} is the colloid concentration that holds at the stagnation line. This balance leads finally to a deposit thickness that reads [5]:

$$e_{LV} \propto \frac{\phi_{stag}}{\phi_c}\frac{J_0^2}{4\theta_S V^2} \tag{8}$$

Unlike e_{HV} at high velocity, this thickness *decreases* with the plate velocity, provided that ϕ_{stag} does not vary too much with V, which should lead to a minimum of the deposed thickness. In Refs. [5,6], we proposed to identify ϕ_{stag} to the concentration of the bulk solution, i.e. the value at infinity ϕ_0, which leads to an exponent of -2 for the scaling of e_{LV}. This description is enough to explain our results, but if one looks more carefully to the data at low velocity in Fig. 2, the exponent -2 overestimates the observed decrease of e_{LV} upon V, and an exponent close to -1 (suggested by the other line added to the graph) would be more reasonable. This observation is consistent with results obtained with other compounds by Faustini [11], Le Berre [12] and Jing et al. [13], the three groups reporting an exponent close to 1 with a better accuracy than our's. This difference of exponent results from the too rough nature of the approximate $\phi_{stag} \approx \phi_0$ used above. Obviously, the concentration of solute increases as the liquid becomes closer and closer to the contact line, which implies the existence of some concentration gradient that we cannot neglect.

4.2. Effect of particle concentration gradients

To evaluate the influence of concentration effects, a simple scaling argument can be built on a slab of liquid, of thickness dx (see Fig. 3b), moving inside a wedge of angle θ_S, at a velocity U toward the contact line, and whose variation of volume per unit length of contact line reads:

$$\delta[hdx] = -\left(\theta U - \theta x\frac{\partial U}{\partial x}\right)\delta t dx = -\theta\delta t\frac{\partial(xU)}{\partial x}dx \tag{9}$$

After combining this with the estimated velocity of the liquid close to contact line, $U \approx J_0/(2\theta\sqrt{x})$, one is led to the conclusion that the slide volume scales as $\sqrt{x(t)}$, and thus that the particle concentration near contact line should in turn scale as:

$$\phi(x) = \phi_0\sqrt{\frac{x_\infty}{x}} \tag{10}$$

where the concentration ϕ_0 holds at the scale of the meniscus (matching with the bulk of the reservoir). Using this expression in the estimate of $\phi_{stag} \approx \phi_0(x_\infty/x_{stag})^{1/2}$ leads finally to the following law ruling the "true" e_{LV}:

$$e_{LV} \propto \frac{\phi_0}{\phi_c}\frac{J_0}{\sqrt{x_\infty}}\frac{x_\infty}{V} \tag{11}$$

in which the new exponent -1 is in better agreement with available data [11,12,14,18] than the previous value -2. Note that this expression, as noticed by Jing et al. [14], can be reached independently by a balance of solute at the level of the whole meniscus:

while the meniscus deposits on the plate of volume of the coated film equal to $Ve_{LV}\phi_c dt$, there is, at the scale of the whole meniscus, a volume of solvent that evaporates equal to $x_\infty(J_0/\sqrt{x_\infty})dt$, and which creates an excess of solute of quantity $\phi_0 x_\infty(J_0/\sqrt{x_\infty})dt$. Balancing this excess of particles with the quantity deposited on the plate leads directly to (11). Finally, in terms of deposit mass, this equation will now read:

$$\frac{\mu}{\phi_m} \propto \frac{\rho l_c^{1/2} J_0}{V} \tag{12}$$

with our typical values $l_c \approx 2\times10^{-3}$ m, $\rho = 1000\,\mathrm{kg\,m^{-3}}$ and $J_0 \approx 10^{-9}\,\mathrm{m^{3/2}\,s^{-1}}$, the prefactor of this law $\rho l_c^{1/2} J_0$ is of order $4.4\times10^{-8}\,\mathrm{kg\,m^{-1}\,s^{-1}}$, which is very close to that assumed for the guide for the eye in Fig. 2b that is equal to $4\times10^{-8}\,\mathrm{kg\,m^{-1}\,s^{-1}}$. Though we do not know the precise numerical prefactor in (12), our modeling recovers thus the right orders of magnitude.

4.3. Influence of particle diffusion

As we have invoked above the existence of concentration gradients of particles, one may wonder whether particle diffusion could also matter at small scale in the problem. The possible influence of particle diffusion can be evaluated by comparing the convection of particles to the diffusion in the horizontal direction, which yields the equivalent of some Peclet number that reads:

$$Pe = \left| \frac{u(x)\phi(x)}{D_{coll}\partial\phi/\partial x} \right| \tag{13}$$

where $D_{coll} \approx k_B T/(6\pi\eta a)$ is the colloid diffusivity deduced from the well known Einstein relation. Close to contact line, as $u(x) \propto J_0/(\theta_S\sqrt{x})$ and $\phi(x) = \phi_0\sqrt{x_\infty/x}$, this quantity varies as:

$$Pe = \frac{J_0}{2\theta_S D_{coll}}\sqrt{x} \tag{14}$$

with the following typical values $J_0 \approx 10^{-9}\,\mathrm{m\,s^{-2}}$, $\theta \approx 5^\circ$, $\eta \approx 10^{-3}\,\mathrm{Pa\,s}$, $a = 50$ nm, $T = 300$ K, one gets for the typical microlength at which $Pe = 1$: $x_{diff} \approx (2\theta_S D_{coll}/J_0)^2 \approx 250$ nm, which is ten times the typical thickness of the deposit revealed in Fig. 1b and not more than five times the colloid diameter. Note also that this diffusive length scale is three orders of magnitude smaller than the capillary length, which leaves a huge range of scales in which the law (10) can hold. It seems that we can thus neglect diffusion of the colloids, but a more careful analysis would be interesting, as we are not so far from conditions where diffusivity could become non-negligible, especially for the smallest size that we used (12 nm).

5. Conclusion

In summary, we have checked experimentally with silica particles deposed on glass our prediction proposed in [5] of the existence of a minimal thickness of colloids deposited on a plate by dip coating, and corrected our model by including the increase of colloid concentration when the liquid reaches the vicinity of the contact line in the low velocity limit. We insist on the fact that this simple approach avoids any use of complicated partial differential equations, and allows one to get a simple understanding of the mechanisms at play here. The behavior that we found, experimentally as well as by a simple modeling, is in agreement with the observations of other groups on different systems [11–15,17,18], and with their own interpretations. It would be interesting to explore experimentally in more details the spatial distribution of colloid concentration in the liquid near the deposition front, to see to what extent a scaling law of the kind (10) could hold. To our knowledge, this has never been done and we are perhaps the first to propose this law. Also, it would be interesting to relate the present transition with the classical Landau–Levich threshold of film entrainment under partial wetting conditions [20,21], and to see if evaporation and deposition introduces a completely different phenomenon, or simply shifts this threshold, for instance via modifications of the reference contact angle due to evaporation [5].

Acknowledgments

We are indebted to discussions with C.-T. Pham, H. Bodiguel, F. Doumenc and B. Guerrier. One of us (G.B.) has benefited from a DGA grant, and this work has been supported by the ANR funding DEPSEC.

References

[1] N.R. Thomson, C.L. Bower, D.W. Mc Comb, Identification of mechanisms, competing with self-assembly during directed colloidal deposition, Journal of Materials Chemistry 18 (2008) 2500–2505.
[2] Y.K. Koh, C.C. Wong, In situ monitoring of structural changes during colloidal self-assembly, Langmuir 22 (2006) 897–900.
[3] D. Qu, E. Ramé, S. Garoff, Dip-coated films of volatile liquids, Physics of Fluids 14 (2002) 1154–1166.
[4] (a) L. Pauchard, M. Adda-Bedia, C. Allain, Y. Couder, On the morphologies resulting from the directional propagation of fractures, Physical Review E 103 (2002) 123–139;
(b) L. Pauchard, Patterns caused by buckle-driven delamination in desiccated colloidal gels, Europhysics Letters 74 (2006) 188.
[5] G. Berteloot, C.-T. Pham, A. Daerr, F. Lequeux, L. Limat, Evaporation-induced flow near a contact line: consequences on coating and contact angle, Europhysics Letters 83 (2008) 14003–14009.
[6] G. Berteloot, Déposition de particules sous évaporation: application au dip-coating, Thesis Univ. Perre et Marie Curie, defended in ESPCI on the 16th November 2009.
[7] E. Rio, A. Daerr, F. Lequeux, L. Limat, Moving contact lines of colloidal suspension in presence of drying, Langmuir 22 (2006) 3186–3191.
[8] R.D. Deegan, O. Bakajin, T.F. Dupont, G. Huber, S.R. Nagel, T.A. Witten, Capillary flow as the cause of ring stains from dried liquids, Nature 389 (1997) 827–828.
[9] R.D. Deegan, O. Bakajin, T.F. Dupont, G. Huber, S.R. Nagel, T.A. Witten, Contact line deposits in an evaporating drop, Phys. Rev. E 62 (2000) 756.
[10] G. Berteloot, A. Hoang, A. Daerr, H.P. Kavehpour, F. Lequeux, L. Limat, Evaporation of a sessile droplet: Inside the coffee stain, Journal of Colloid and Interface Science 370 (2012) 155.
[11] M. Faustini, B. Louis, P.A. Albouy, M. Kuemmel, D. Grosso, Preparation of sol–gel films by dip-coating in extreme conditions, Journal of Physical Chemistry C 114 (2010) 7637–7645.
[12] M. Le Berre, Y. Chen, D. Baigl, From convective assembly to Landau–Levich deposition of multilayered phospholipid films of controlled thickness, Langmuir 25 (2009) 2554–2557.
[13] H. Bodiguel, F. Doumenc, B. Guerrier, Stick-slip patterning at low capillary numbers for an evaporating colloidal suspension, Langmuir 26 (2010) 10758–10763.
[14] G. Jing, H. Bodiguel, F. Doumenc, E. Sultan, B. Guerrier, Drying of colloidal and polymer solutions near the contact line: deposit thickness at low capillary number, Langmuir 26 (2010) 2288–2293.
[15] D.D. Brewer, T. Shibuta, L. Francis, S. Kumar, M. Tsapatsis, Coating process regimes in particulate film production by forced-convection-assisted drag out, Langmuir 27 (2011) 11660–11670.
[16] (a) L.D. Landau, V.G. Levich, Dragging of a liquid by a moving plate, Acta Physicochimica USSR 17 (1942) 42–54;
(b) B. Derjaguin, Thickness of liquid layer adhering to walls of vessels on their emptying and the theory of photo- and motion-picture film coating, Doklady Academy of Sciences USSR 39 (1943) 13–19.
[17] A.S. Dimitrov, K. Nagayama, Continuous convective assembling of fine particles into two-dimensional arrays on solid surfaces, Langmuir 12 (1996) 1303–1311.
[18] J.J. Diao, M.G. Xia, A particle transport study of vertical evaporation-driven colloidal deposition by the coffee-ring theory, Colloids and Surfaces A 338 (2009) 167–170.
[19] M. Ghosh, F. Fan, K.J. Stebe, Spontaneous pattern formation by dip coating of colloidal suspensions on homogeneous surfaces, Langmuir 23 (2007) 2180–2183.
[20] see for instance D. Bonn, J. Eggers, J. Indekeu, J. Meunier, E. Rolley, Wetting and spreading, Reviews of Modern Physics 81 (2009) 739, section G, and references therein.
[21] J.H. Snoeijer, G. Delon, M. Fermigier, B. Andreotti, Avoided critical behavior in dynamically forced wetting, Physical Review Letters 96 (2006) 174504.